Preliminary parametric study of a tidal energy device using an open-source CFD tool

Pilechi, Abolghasem; Ferguson, Sean; Ghodoosipour, Behnaz; Cornett, Andrew; Bateham, Laird

Publisher's version / Version de l'éditeur:

Proceedings of ISOPE 2021, 2021-06-20

Preliminary parametric study of a tidal energy device using an open-source CFD tool

Abolghasem, Pilechi
National Research Council Canada
Ottawa, Ontario, Canada
Sean Ferguson
National Research Council Canada
Ottawa, Ontario, Canada
Behnaz Ghodoosipour
National Research Council Canada
Ottawa, Ontario, Canada
Andrew Cornett
National Research Council Canada
Ottawa, Ontario, Canada
Laird Bateham
Yourbrook Energy Systems Ltd.
Queen Charlotte, British Columbia, Canada

ABSTRACT
Simultaneous advancements in high-performance computing technologies (HPC) and fluid dynamics science have set the stage for practical computational fluid dynamics (CFD) modelling of complex real-life problems including fluid-structure interaction. The presented research summarizes the capabilities of the OpenFOAM CFD toolbox to facilitate design optimization of an innovative tidal energy device. Numerical simulations were conducted for different environmental conditions and operating scenarios to characterize the flows through the device. The influence of changing the number of turbine blades as well as their submergence depth in the incident flow was tested through a series of 2D numerical simulations which consider the dynamics of the rotary component of the system. The results of the simulations were used to investigate potential strategies for design optimization, ultimately improving efficiency.

KEY WORDS: CFD; tidal energy device; numerical modelling; OpenFOAM

INTRODUCTION

Diminishing fossil fuel resources, and an increased understanding of the environmental impacts associated with fossil fuel power generation, has brought increasing attention to renewable energy resources such as hydro power. Water wheels are one of the oldest forms of hydropower conversion technologies and have historically been used to extract energy from stream flows (Poncelet, 1843). In general, there are four types of water wheels: undershot, overshot, breast-shot, and stream water wheels. Detailed information about each type of water wheel and their characteristics can be found in references Nguyn et al. (2018), and Tevata and Inprasit (2011). Stream water wheels (Fig. 1) are mainly used for harnessing energy from surface flows and are generally regarded as eco-friendly devices owing to their relatively low impact on the ambient environment. Recent improvements in the efficiency of water wheel systems has motivated their application as a means for generating electricity for remote sites that are isolated from large-scale transmission networks (Bozhinova et al., 2013).

The performance and efficiency of a water wheel system depends on a number of different factors including, for example: the capability of the wheel to extract and transfer the available hydrokinetic energy in the ambient flow to the wheel shaft, the performance of the power take-off system, and the structural resilience of system components. Previous research has been conducted on the development and optimization of water wheel systems using analytical, numerical, and experimental approaches. In general, the main objective of previous research has been to inform design optimization in such a manner that maximizes energy extraction and minimizes construction and maintenance costs. Some studies have investigated design of the platform which the wheel is mounted on (Baker et al., 2015; Batten and Batten, 2015), and others have focused on the wheel characteristics such as the number of blades and their shape (Tevata and Inprasit, 2011; Quaranta and Revelli, 2015; Vidali *et al.*, 2016; Quaranta and Revelli, 2016).

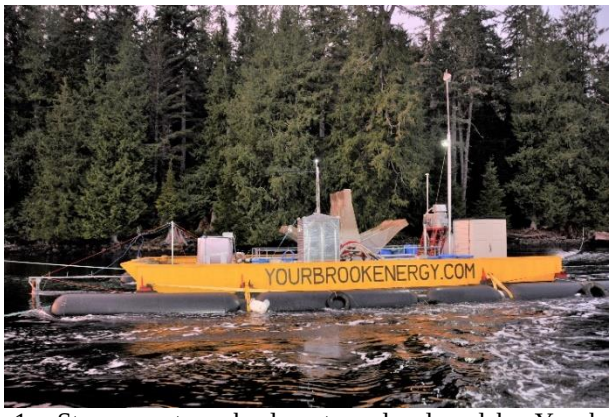

Fig. 1. Stream water wheel system developed by Yourbrook Energy Systems Ltd. (photograph credit: National Research Council Canada)

Numerical modelling, in particular CFD modelling, has been extensively used for performance assessment and design optimization of different types of hydro power equipment. Most previous CFD modelling research on water wheels has been conducted using commercial CFD tools. References (Sam, 1990; Quaranta and Revelli , 2017; Akinyemi and Liu, 2015) have applied CFD modelling techniques to inform optimization of water wheel systems using ANSYS FLUENT software.

Yourbrook Energy Systems Ltd. (hereafter referred to as Yourbrook) is a Canadian firm based in Haida Gwaii, British Columbia, Canada (www.yourbrookenergy.com). Yourbrook has developed, and continues to refine, a conceptual tidal energy device that is capable of harnessing energy over a range of tidal flows. The conceptual device combines surface-mounted water wheel technology with pumped-storage hydropower, with the objective of facilitating continuous power generation throughout the tidal cycle, including periods of slack tide. The conceptual device uses an intricate pumping system that is driven by the rotational motion of the wheel. The pumping system uses variable displacement technology that allows pumping (and power generation) to be achieved over a range of rotational speeds and operating conditions. To date, Yourbrook has constructed a working prototype device (Fig. 1) to support testing and inform technology development and optimization.

The objective of the research described in this paper was to examine the capabilities of the OpenFOAM CFD tool box to model the water wheel component of the hydrokinetic energy prototype device manufactured by Youbrook (Fig. 1). Two-dimensional CFD modelling was applied to simulate the water wheel component of Yourbrook's current prototype device. In addition, the model was used to investigate potential strategies for design optimization through parametric adjustment of several geometric wheel characteristics. The parametric investigation was limited to geometric adjustment of the wheel and subsequent assessment of wheel shaft power. The pumping system (i.e. the power take-off system) employed in Yourbrook's tidal energy technology was not investigated. Similarly, the scope of the research did not include investigation of structural resilience or economic viability of the tested designs.

MODELLING

This section presents a summary of the numerical modelling process, including a description of the modelled wheel designs and the details of the CFD model set up. All of the simulations performed in this study were conducted using OpenFOAM which is an open source CFD tool box. In order to model the free surface, a multiphase solver of OpenFOAM named InterFOAM was employed. The InterFOAM module solves the Reynolds-Averaged Navier-Stokes (RANS) equations for incompressible fluids. InterFOAM is an OpenFOAM solver that is typically used to support simulation of fluid-structure interactions that involve dynamic variation of the free surface. The solver uses volume of fluid (VOF) techniques to support modelling of the free surface.

The rotational motion of the wheel was implemented into the numerical model in order to enhance the realism of the simulations. This was achieved by applying the Arbitrary Mesh Interface (AMI) technique in OpenFOAM which enables simulation across disconnected, adjacent domains. Using this technique, the domain was split into static and moving (rotating) domains. The mesh for each of the domains was generated separately and the domains were coupled through patch boundaries. The CFD model was initially set up to replicate the current geometry of the prototype wheel provided by Yourbrook (test case T1 in Table 1). Hydraulic parameters such as water depth and flow speed were specified to match observations recorded during a site visit and field measurement program (not discussed in this paper). Blade "tip speed ratio" (TSR) is a non-dimensional parameter defined by (Mehmood *et al.,* 2012) as:

$$TSR = \frac{R\omega}{U} \qquad (1)$$

where R is the wheel radius, ω is the angular speed of the wheel (rad/s) and U is the undisturbed flow velocity (m/s). A constant TSR of 0.44 was maintained to match the operational controls currently employed by Yourbrook. To evaluate the influences of the ambient flow speed and the rotational speed on performance, the original design was modelled with two additional flow speeds (T2, T3) and rotational speeds (T4, T5).

In addition to the mentioned test cases, multiple design factors were also investigated in this study including the number of wheel blades and the diameter of the wheel. A summary of all of the CFD simulations conducted in this study and their configuration parameters, including the number of the wheel blades (N), average ambient water depth (H), TSR, average flow speed (U), and diameter of the wheel (D), is provided in Table 1. One of the main geometrical characteristics that influences performance and efficiency is the submergence depth of the blades during operation. This parameter is represented in Table 1 by immersion ratio (Ir) which is the ratio between the blade dip depth at maximum submergence (I) and the radius of the wheel (R) (see Fig. 2).

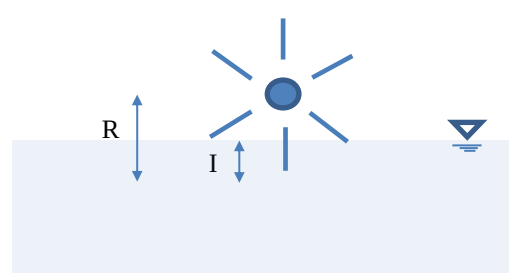

Fig. 2. Schematic illustration of the CFD model

All of the models developed for this study were constructed using a Hexahedral mesh system. The mesh generation was carried out using SnappyHexMesh, a built-in mesh generator of OpenFOAM that facilitates the generation of geometry-conforming Hexahedron meshes. As discussed before, the mesh consisted of two components corresponding to the stationary and the rotating (wheel) parts of the model (see Fig. 3). Sensitivity analysis was conducted on the mesh in

order to identify the resolution and configuration required to provide a reasonable balance between computational speed and accuracy. The version of the model mesh used to produce the results reported here was composed of 105,617 elements with a minimum cell size of 5cm in the rotating zone. The grid resolution was chosen through an iterative process which involved comparing the impact of different element sizes on simulation results. Using the selected grid configuration, 100 seconds of parallel simulations for 105,617 elements could be achieved over a 4 day duration using 4 cores. A sensitivity analysis indicated that there was less than 7% discrepancy between shaft power estimates computed using the selected grid configuration and a coarser grid configuration with a minimum cell size of 10cm.

Table 1. Test matrix of CFD simulations

N	Test	H (m)	TSR	Ir	U(m/s)	D(m)
	T6	6	0.44	0.56	1.6	5
	T7	6	0.44	0.6	1.6	5
5	T9	6	0.44	0.64	1.6	7
	TT6	6	0.68	0.56	1.6	5
	TT7	6	0.68	0.6	1.6	5
	T8	6	0.44	0.4	1.6	5
	T2	6	0.44	0.56	1.45	5
	T3	6	0.44	0.56	1.9	5
	T10	6	0.44	0.6	1.6	5
6	T1	6	0.44	0.56	1.6	5
	T4	6	0.47	0.56	1.6	5
	TT8	6	0.68	0.4	1.6	5
	TT1	6	0.68	0.56	1.6	5
	T5	6	0.78	0.56	1.6	5

A two-level boundary layer was applied on the surface of the blades in order to improve numerical stability of the model. The distance between the rotating and stationary parts of the mesh was specified to ensure a smooth transition between the two zones (see Fig. 3).

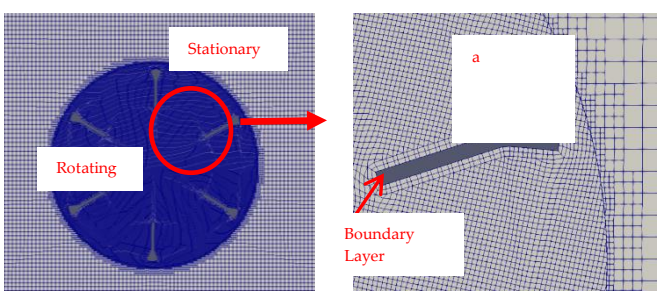

Fig. 3. Application of AMI technique and Hexahedral mesh system in the CFD model

The 2D numerical model domain was built as a straight channel with a length of 50m (*Lx*) and a depth of 13m (*Ly*). The flow was introduced into the domain by prescribing a constant flow rate boundary condition at the upstream boundary. Flow exits the domain through an outlet boundary at the downstream end of the domain (see Fig. 4). A summary of the boundary conditions used in the OpenFOAM model is provided in Table 2 where *P* is the dynamic pressure, *K* is the turbulent kinematic energy, *ε* is the dissipation rate, '*nut*' is the turbulent eddy viscosity, and *Alpha* denotes the fluid fraction parameter in the VOF method.

The average power transferred from the flow to the wheel shaft (hereafter referred to as "shaft power") was computed for each simulation identified in Table 1 and was used as a metric to evaluate performance. The shaft power was calculated from model results as a function of torque and rotational speed using the following equation:

$$P = T * \omega \qquad (2)$$

where *T* is the total torque exerted on the wheel by the water flow. The kinetic power available in the incident flow was also computed for each test case using the following equation

$$P = \frac{1}{2}\rho A U^3 \qquad (3)$$

where ρ represents the density of the ambient water (assumed equal to 1015 kg/m^3) and *A* represents the swept area per unit width, as the model is 2D, of the wheel through the flow. For each test case, efficiency was computed as the ratio between the shaft power of the wheel and the power available in the flow. The reported efficiency values do not include the performance of the power take-off system and, therefore, do not reflect the overall efficiency of the tidal energy device.

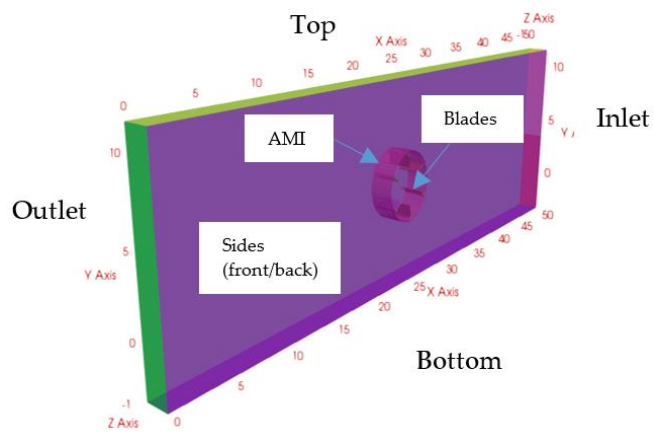

Fig. 4. Schematic illustration of the CFD model boundary patches

Table 2. Applied boundary condition in the OpenFOAM model

	U	P	K	ε	nut	Alpha
Inlet	V.I [a]	F.F [b]	Z.G [c]	Z.G	Z.G	V.H [d]
Outlet	I.O [e]	F.V [f]	Z.G	Z.G	Z.G	Z.G
Top	P.I [g]	T.P [h]	Z.G	Z.G	Z.G	Z.G
Bottom	S [i]	F.F	Z.G	Z.G	Z.G	Z.G
AMI	C.A [j]	C.A	C.A	C.A	C.A	C.A
Blades	M.W [k]	F.F	Z.G	Z.G	Z.G	Z.G
Sides	E [l]	E	E	E	E	E

[a] Variable Height Flowrate Inlet Velocity
[b] Fixed Flux Pressure
[c] Zero Gradient
[d] Variable Height Flow Rate
[e] Inlet Outlet
[f] Fixed Value
[g] Pressure Inlet Outlet
[h] Total Pressure
[i] Slip
[j] Cyclic AMI
[k] Moving Wall Velocity
[l] Empty

RESULTS

This section summarizes the results of the numerical simulations. The impacts of different numerical, hydraulic, and geometric parameters on the hydrodynamics and performance of the wheel were investigated.

In order to inform improvement of the wheel design, a series of simulations were conducted in which several parameters of the wheel design were adjusted including the number of the blades, the immersion ratio, the rotational speed, the wheel diameter, and the incident flow speed. For each of the simulations, the changes in streamwise velocity along the main flow direction (x), the torque applied on the water wheel, and the shaft power of the wheel were computed and analyzed. Shaft power was computed using equation (2) and was used as a metric to evaluate performance of the wheel. All of the data presented in this paper were computed based on model outputs averaged over a duration of 50s after reaching a steady condition. The shaft power values were normalized with respect to the area swept by unit width of a submerged paddle during one full rotation (swept area) to facilitate comparison amongst different simulations. The average torque applied on the wheel by the water and the average shaft power for each case are summarized in Table 3. Fig. 5 presents snapshots of the flow stream lines at four different phases of wheel rotation for simulation T1.

Table 3. Applied torque on the wheel and the resulting shaft power for simulated cases

N	Test	TSR	Torque (kN.m)	Power (kW)	Normalized power (kW/m^2)	ΔU (m/s)	Efficiency (%)
	T6	0.44	7.43	2.08	1.49	0.73	36
	T7	0.44	8.20	2.29	1.53	0.77	37
5	T9	0.44	14.34	4.01	1.79	0.3	43
	TT6	0.68	3.51	1.55	1.11	0.38	27
	TT7	0.68	3.63	1.59	1.06	0.32	25
	T8	0.44	4.07	1.14	1.14	0.44	27
	T2	0.44	4.83	1.20	0.86	0.52	28
	T3	0.44	12.35	3.45	2.46	0.60	35
	T10	0.44	8.71	2.44	1.63	0.79	39
6	T1	0.44	7.72	2.16	1.54	0.70	37
	T4	0.47	7.68	2.30	1.64	0.79	40
	TT8	0.68	1.59	0.70	0.70	0.27	17
	TT1	0.68	3.29	1.44	1.03	0.43	25
	T5	0.78	1.04	0.52	0.37	0.23	9

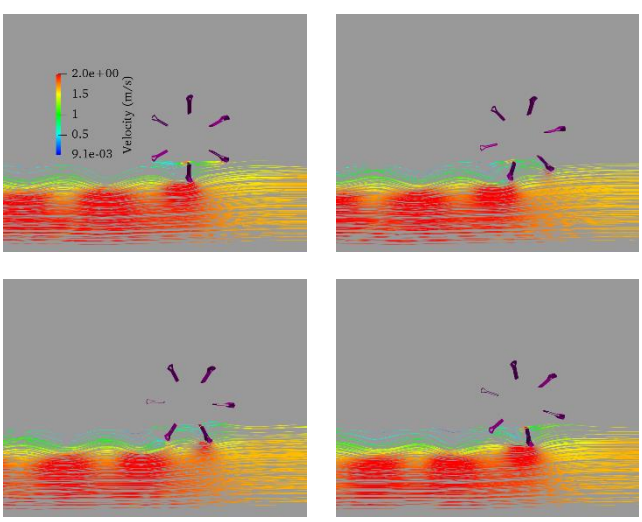

Fig. 5. Modelled flow streamlines around the wheel at four different time steps for simulation T1

Time-averaged velocities were computed at 10 points that are symmetrically distributed at ± D_0, ± 1.5D_0, ± 2D_0, ± 2.5D_0 with respect to the center of the wheel (0,0), where D_0 represents the diameter of the current wheel design (5m). The data are shown in Fig. 6. The data indicate that changes in the wheel design have a small, but noticeable, impact on upstream velocity. However, different wheel designs produce significantly different downstream velocities. Also, for a given blade number and rotational speed, immersion ratios that produced greater change in velocity across the wheel (ΔU in Table 3) were associated with higher efficiency in most cases. The influence of different wheel designs on shaft power is discussed in the following sections.

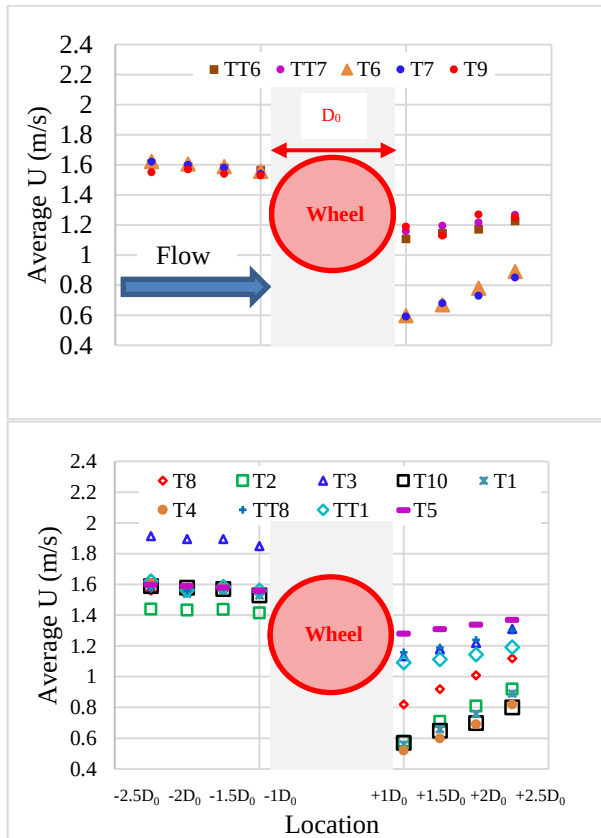

Fig. 6. Average streamwise velocity for simulations listed in Table 1; five-blade wheel design (top), six-blade design (bottom)

Influence of Turbulence

In addition to the simulations listed in Table 1, cases T1 and TT1 were simulated with both laminar and turbulent configurations to investigate the impact of turbulence on the modelled shaft power. Fig. 7 compares the shaft power predicted by the CFD model for the laminar and turbulent flow configurations. The computed shaft power is greater in the laminar cases. These results suggest that turbulence dissipates some of the energy available in the flow, resulting in less power extraction by the wheel. All of the other simulations in this study were conducted using the standard k-ε turbulence model.

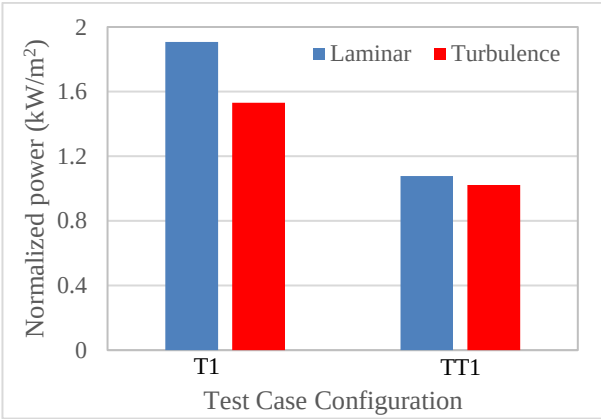

Fig. 7. Influence of turbulence model on the modelled shaft power

Base Case

A base case simulation was conducted in which the configuration of Yourbrook's prototype device was replicated (T1 in Table 1) in order to assess the power extraction capacity of the existing design. In this analysis the kinetic power available in the incident flow was computed based on an ambient flow speed of 1.6m/s, which corresponds to an available power of 5.8kW. Under these flow conditions, the shaft power of the wheel, as predicted in the CFD model, equals 2.16kW. This suggests that the wheel is capable of transferring approximately 37% of the kinetic power available in the flow to the shaft.

Number of Blades

The influence of the number of the blades on power extraction was investigated by comparing results from six simulations as shown in Fig. 8. In four of these simulations (T1, T6, T7, T10), the TSR of the wheel was 0.44. However, the immersion ratio in T7 and T10 was 7% greater than in T1 and T6. The TSR in the other two simulations (TT1 and TT6) was 0.68 (55% faster). The results show that, when a lower rotational speed was modelled (TSR = 0.44), the six-blade wheel produced approximately 4% more power than the five-blade wheel. Conversely, when a faster rotational speed was modelled (TSR = 0.68), the five-blade wheel outperformed the six-blade wheel.

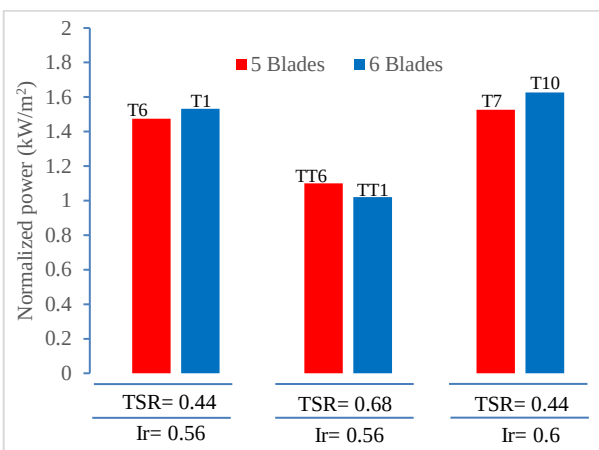

Fig. 8. Influence of number of wheel blades on shaft power

Rotational Speed

The rotational speed of the wheel is one of the primary parameters influencing power production of a stream water wheel system. The majority of the simulations in this study were conducted using a TSR of 0.44 based on the recommendations of Pinard (2011) derived through a theoretical assessment of Yourbrook's water wheel technology. However, the optimal TSR recommended by Pinard (2011) was calculated based on a hypothetical wheel and blade geometry that is different than Yourbrook's current, prototype design. Pinard (2011) assumed an eight-blade wheel constructed with solid blades such that water cannot flow over top of submerged blades. Furthermore, the methods applied by Pinard (2011) did not consider complex dynamic interaction of the wheel with the ambient flow. Therefore, device performance was also investigated numerically for three other TSR values equal to 0.47, 0.68 and 0.78; and the results are shown in Fig. 9. The shaft power of the original design improved by 8% with TSR = 0.47 compared to results with TSR = 0.44. Further investigation is required to identify the optimal rotational speeds for different configurations.

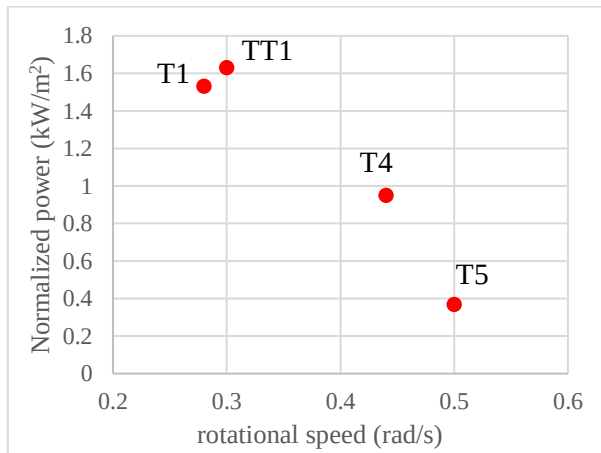

Fig. 9. Influence of wheel rotational speed on shaft power

Immersion Ratio

Theoretically, the maximum power generated by a water wheel is directly linked to the submergence depth of the blade, and by extension, the swept area. This parameter was represented in this study by the immersion ratio (Ir). Previous studies have shown that immersion ratio can significantly change the power production of a stream water wheel system (Tevata and Inprasit, 2011). Four different immersion ratios were modelled to investigate the influence of blade submergence depth. Fig. 10 compares the shaft power normalized by the swept area in these four simulations. In general, for a given combination of blade-number and TSR, normalized power was positively correlated with immersion ratio. However, for test cases that included a 5-bladed wheel and a TSR of 0.68 (TT6 and TT7), a decrease in normalized power was observed with increasing immersion ratio.

One simulation, T9, was conducted to evaluate the impact of increasing the wheel diameter, increasing immersion ratio, and repositioning the wheel above the water surface. Unlike all other simulations, which considered a wheel diameter of 5m, a 7m diameter 5-bladed wheel was modelled in simulation T9. The geometry of the solid portion of the wheel blades for T9 was identical to the geometry of the solid portion of the wheel blades for all other simulations. The "spoke" length of each blade in T9 was simply increased to create a larger wheel diameter.

The computed normalized shaft power for simulation T9 was greater than all other cases run with the base ambient velocity (1.6m/s). It is difficult to conclude whether the increase in performance is due to the orientation of submerged blades, the increase in swept area, the increased radius and implications on torque, or a combination of the above.

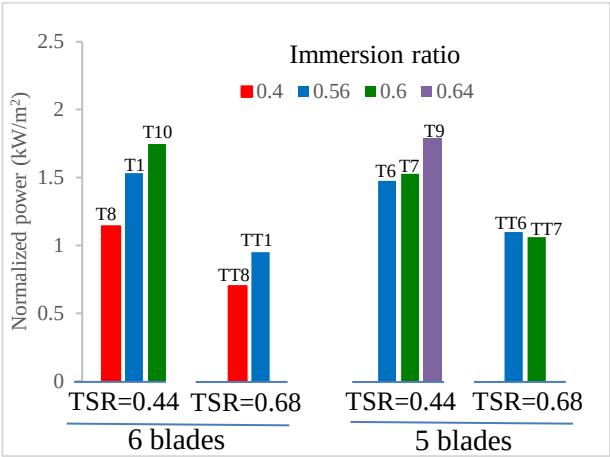

Fig. 10. Influence of immersion ratio on shaft power

Flow Speed

In addition to the base case (T1) condition, with an ambient flow speed of 1.6m/s, the performance of Yourbrook's water wheel device was also investigated at one slower (1.4m/s) and one faster (2m/s) ambient flow speed. Ambient flow speeds of 1.4m/s and 2.0m/s correspond to a 12.5% decrease and a 25% increase in flow speed when compared to the base case, respectively. The model results, plotted in Fig. 11, indicate a 44% decrease in shaft power when flow speed is reduced by 12.5%, and a 62% increase in shaft power when flow speed is increased by 25%. These results suggest that shaft power increases with increasing flow speed, as expected. These results also suggest that the relationship between shaft power and flow speed is roughly linear over this range for a consistent tip speed ratio.

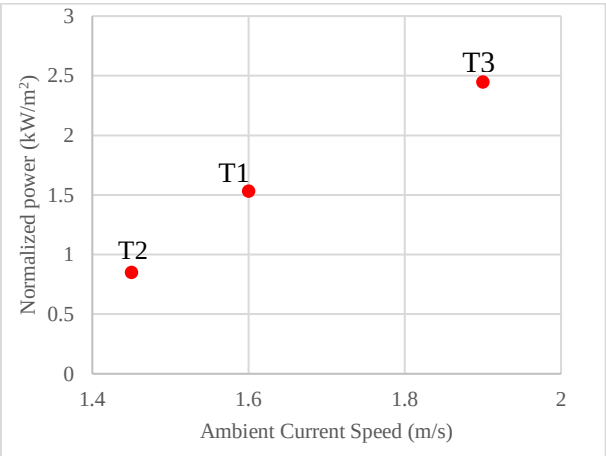

Fig. 11. Shaft power under different flow speeds

CONCLUSIONS

In this study the capabilities of the OpenFOAM CFD tool box were applied in a preliminary parametric investigation of the water wheel component of Yourbrook Energy Systems' tidal energy device. It is anticipated that the findings from this research will inform future strategies for design optimization and operational procedures to improve power output and efficiency.

One simulation was conducted to assess Yourbrook's existing prototype design. The model results suggest that, at an ambient flow speed of 1.6m/s, the current design transfers energy from the tidal flow to the wheel shaft with an efficiency of approximately 37%.

Following assessment of the original design, additional CFD simulations were conducted in which various alternative wheel designs and rotation speeds were modelled. A number of parameters were varied to assess their impact on performance, including: blade submergence depth, the number of blades, wheel diameter, wheel rotational speed, and the incident flow speed. The shaft power of the wheel for each case was calculated and the influence of each parameter was investigated.

A six-bladed wheel delivered better performance than a five-bladed wheel for lower rotational speeds (TSR = 0.44). Increasing blade submergence depth improved normalized shaft power for all six-bladed wheel designs within the realm of tested conditions. Similarly, increasing blade submergence depth improved normalized shaft power for five-bladed wheel designs with a tip speed ratio of 0.44, but caused a reduction in normalized shaft power for six-bladed wheel designs with a tip speed ratio of 0.68. Changing the five-bladed wheel diameter from 5m to 7m, in addition to increasing the submergence depth, resulted in the greatest shaft power (4.01kW) and efficiency (43%) among the modelled cases. These findings suggest that typical design parameters, such as the immersion ratio and number of blades, should not be relied upon individually as an indicator of system performance. Yourbrook's design does not resemble a traditional water wheel where the swept area is completely blocked by solid blades. The open space between the solid portion of each blade and the axle allows water to flow over top of the submerged blades, which makes the water-blade interaction more complex and difficult to predict using simple methods. Simulation results for different rotational speeds also suggest that the previously recommended TSR value (0.44) may not be the optimal value for all flow conditions and wheel designs.

The OpenFOAM CFD model showed acceptable performance in simulating the operation of the hydrokinetic device examined in this study, particularly in modelling the dynamics of the rotary component of the system. The trends observed in model results, in response to parameter adjustments, suggest that the model can be used as a practical means for optimization of this type of system. The model performance can be further improved by investigating the influence of different turbulence models, and by validating model results through comparison with field data or data obtained through physical modelling.

ACKNOWLEDGEMENTS

The authors gratefully acknowledge funding for this research from Yourbrook Energy Systems Ltd., NRC, and the Industrial Research Assistance Program.

REFERENCES

Baker, S., Cornett, A., Kluijver, M. (2015). "3D Modelling and Optimization of a Hydrokinetic Power Generation Barge," *11th European Wave and Tidal Energy Conference*.

Batten, W.M.J., Batten, G.U. (2015). " Potential for using the floating body structure to increase the efficiency of a free stream energy converter,"

34th World Congress of the International Association for Hydro-Environment Research and Engineering: 33rd Hydrology and Water Resources Symposium and 10th Conference on Hydraulics in Water Engineering, Engineers Australia, pp. 23-64.

Bozhinova, S., Kisliakov, D., Müller, G., Hecht, V., Schneider, S. (2013). "Hydropower converters with head differences below 2· 5 m," *ICE: Energy*, vol. 166, no. 3, pp. 107-119.

Mehmood, N., Liang, Z., Khan, J. (2012) "Diffuser augmented horizontal axis tidal current turbines," Res J Applied Sci Eng & Tech, 18: 3522–3532.

Nguyn, M.H., Jeong, H., Yang, C. (2018). "A study on flow fields and performance of water wheel turbine using experimental and numerical analyses." *Sci. China Technol.* Sci. 61: 464. https://doi.org/10.1007/s11431-017-9146-9

Pinard. J.p., Gillespie, G., (2011) "An Engineering Analysis of a Tidal/Hydro System for Makii Point Power Project".

Poncelet, J. V. (1843). "Memoria sulle ruote idrauliche a pale curve, mosse di sotto, seguita da sperienze sugli effetti meccanici di tali ruote," Translated by Errico Dombrè, *Dalla tipografia Flautina, Napoli*.

Tevata, A., Inprasit, C. (2011). "The effect of paddle number and immersed radius ratio on water wheel performance," *Energy Procedia*, vol. 9, pp. 359-365, 2011.

Quaranta, E., Revelli, R. (2015). "Performance characteristics, power losses and mechanical power estimation for a breastshot water wheel." *Energy*, 87: 315–325

Quaranta, E., Revelli, R. (2016). "Optimization of breastshot water wheels performance using different inflow configurations", *Renewable Energy*, 97, 243–251.

Quaranta, E., Revelli, R. (2017) "CFD simulation to optimize the blade design of water wheels," *Drinking Water Engineering and Science*, vol. 10, no. 1, pp. 27-32.

Sam, Al (1990). "Water wheel CFD simulations" *Master thesis*, Division of Fluid Mechanics Department of Energy Sciences, Faculty of Engineering, Lund University, Sweden.

Vidali, C., Fontan, S., Quaranta, E., Cavagnero, P., Revelli, R. (2016). "Experimental and dimensional analysis of a breastshot water wheel," *Journal of Hydraulic Research*, vol. 54, pp. 473–479.